

# Irregular wave dynamics driven by a random force within the Burgers equation

Author

**Abstract:** In this article, we study the classical Burgers equation as a model for random fields. First, we consider initial data defined as a sum of harmonics with random phases and compute the blow-up time. Several simulations are performed, revealing that, while the critical blow-up time is approximately distributed according to a Gaussian law, the statistical tests reject the normality hypothesis. For the viscous case, we analyze waves driven by a random force. Using the Cole-Hopf transformation, the averaged wave field is computed numerically. Through a change of variables, we demonstrate that randomness primarily affects the phase of the wave field. Assuming the phase follows a uniform distribution, we show that the averaged field spreads and diminishes over time.

**Keywords:** Burgers equation, wave breaking, random waves, stochastic force.

## 1. Introduction

Several models are used to describe the dynamics of nonlinear waves in fluids. While more complex models may better capture real-world phenomena, they also introduce significant challenges in solving the associated nonlinear partial differential equations, whether analytically or numerically. Dispersive equations, such as the Korteweg-de Vries and Benjamin-Ono equations, serve as excellent prototypes for studying solitons and algebraic solitons. Although these equations can also be employed to model random wave fields, the results are inherently limited to numerical approaches [12]. The Burgers equation [3] although simple, it carries two important mechanism in nonlinear physics, nonlinearity and viscosity

$$u_t + uu_x = \nu u_{xx}, \quad (1.1)$$

where,  $u = u(x, t)$  represents the wave field at the position  $x$  and time  $t$ , and  $\nu$  is a constant that carries the information of the kinematic viscosity (Reynolds viscosity) of the fluid. Such equation appears widely in the literature for studying shock waves [3] which also appear in the study of plasma physics [1, 15, 17, 18] and hydrodynamics [19, 20, 21]. Besides, it represents the dispersionless limit of significant equations in physics, such as the Korteweg-de Vries (KdV) equation, the Benjamin-Ono (BO) equation, the Whitham equation, and others [4, 23, 2, 22, 7, 5, 16]. Although the Burgers equation has been extensively studied in the literature, it continues to be a subject of ongoing research in the field of nonlinear physics [13, 9].

The aim of this work is to examine the propagation of a random initial condition within the Burgers equation (1.1). We explore several scenarios. First, in the inviscid limit ( $\nu \rightarrow 0$ ), we compute the average time for wave breaking and demonstrate that the critical time follows a distribution closely approximated by a normal distribution. Additionally, in the viscous case, we apply the Cole-Hopf transformation to determine the exact solution of the Burgers equation and analyze the impact of a random force on the wave field. Our results show that the mean wave field attenuates and spreads over time.

## 2. Modeling equations

The initial value problem for the Burgers equation is

$$\begin{cases} u_t + uu_x - \nu u_{xx} = 0, \\ u(x, 0) = u_0(x). \end{cases} \quad (2.1)$$

To model the initial wave field, we consider an irregular wave field represented by a Fourier series with  $N$  harmonics

$$u_0(x) = \sum_{i=1}^N \sqrt{2S(k_i)\Delta k} \cos(k_i x + \varphi_i), \quad (2.2)$$

where  $S(k)$  is the initial power spectrum,  $k_i = i\Delta k$  is the wave number, with  $\Delta k$  being the sampling wave number, and  $\varphi_i$  is a random variable uniformly distributed over the interval  $(0, 2\pi)$ , which adds randomness to the problem. In this study, we assume a Gaussian-shaped wavenumber power spectrum

$$S(k) = Q \exp\left(-\frac{1}{2} \frac{(k - k_0)^2}{2K^2}\right), \quad (2.3)$$

where  $Q$  and  $K$  are positive constants, and  $k_0$  represents the central wavenumber. For numerical studies on dispersive equations, we refer the reader to [12] and the references therein. In what follows we take  $N = 256$  harmonics with a step size  $\Delta k = 0.023$  in the wavenumber domain,  $Q = 1$  for the spectrum amplitude and  $K = 0.18$  for the spectrum width.

## 3. Results

### 3.1. The inviscid problem ( $\nu = 0$ )

To solve the inviscid Burgers equation ( $\nu = 0$ ) given by

$$u_t + uu_x = 0, \quad (3.1)$$

with an initial condition  $u(x, 0) = u_0(x)$ , we apply the method of characteristics. Along each characteristic curve, the function  $u$  remains constant, which implies

$$\frac{du}{dt} = u_t + uu_x = 0. \quad (3.2)$$

Therefore, we have

$$u(x, t) = u_0(s), \quad (3.3)$$

where  $s$  is the initial parameter of the characteristic, and it satisfies the equation

$$x = s + u_0(s)t. \quad (3.4)$$

Next, we introduce the function  $z(s, t) = u_0(s)$ . Using the Fourier representation of the initial condition  $u_0(x)$ , we obtain

$$z(s, t) = \sum_{i=1}^N \sqrt{2S(k_i)\Delta k} \cos(k_i s + \varphi_i) = h(s), \quad (3.5)$$

where  $S(k)$  is the initial power spectrum defined in (2.3), and  $\varphi_i$  is a random variable uniformly distributed over the interval  $(0, 2\pi)$ . The wave profile can now be visualized in the coordinates

$$(x, t, z) = (s + th(s), t, h(s)). \quad (3.6)$$

Finally, for several realizations of the random phase vector  $\varphi \in \mathbb{R}^M$ ,  $\varphi_m \sim U[0, 2\pi]$ , we compute the characteristic time  $\bar{t}_c$ , defined as

$$t_c = -\frac{1}{\min_s h'(s)}. \quad (3.7)$$

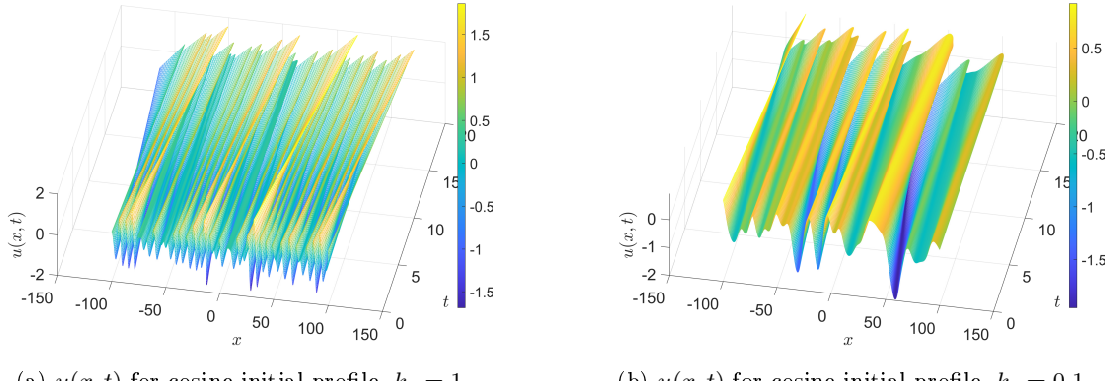


Figure 1: Comparison of  $u(x, t)$  for cosine initial profiles with  $k_0 = 1$  (left) and  $k_0 = 0.1$  (right).

The results of the simulations are illustrated in the following figures. Figure 1a shows the wave field for moderate wavelengths ( $k_0 = 1$ ), while Figure 1b presents the corresponding results for long waves ( $k_0 = 0.1$ ). In both cases, we observe that the wave field experiences an overturn, indicating a gradient catastrophe; in other words, the gradient of the solution blows up in finite time.

In order to determine a distribution law for the wave-breaking time ( $t_c$ ), a series of Monte Carlo simulations were performed, and the results are displayed in the histograms in Figures 2a, 2b, 2c, and 2d. These figures illustrate the empirical distributions of the critical time  $t_c$  for  $M = 2000$ ,  $M = 4000$ ,  $M = 6000$ , and  $M = 8000$  simulations, respectively, with  $k_0 = 0.01$ .

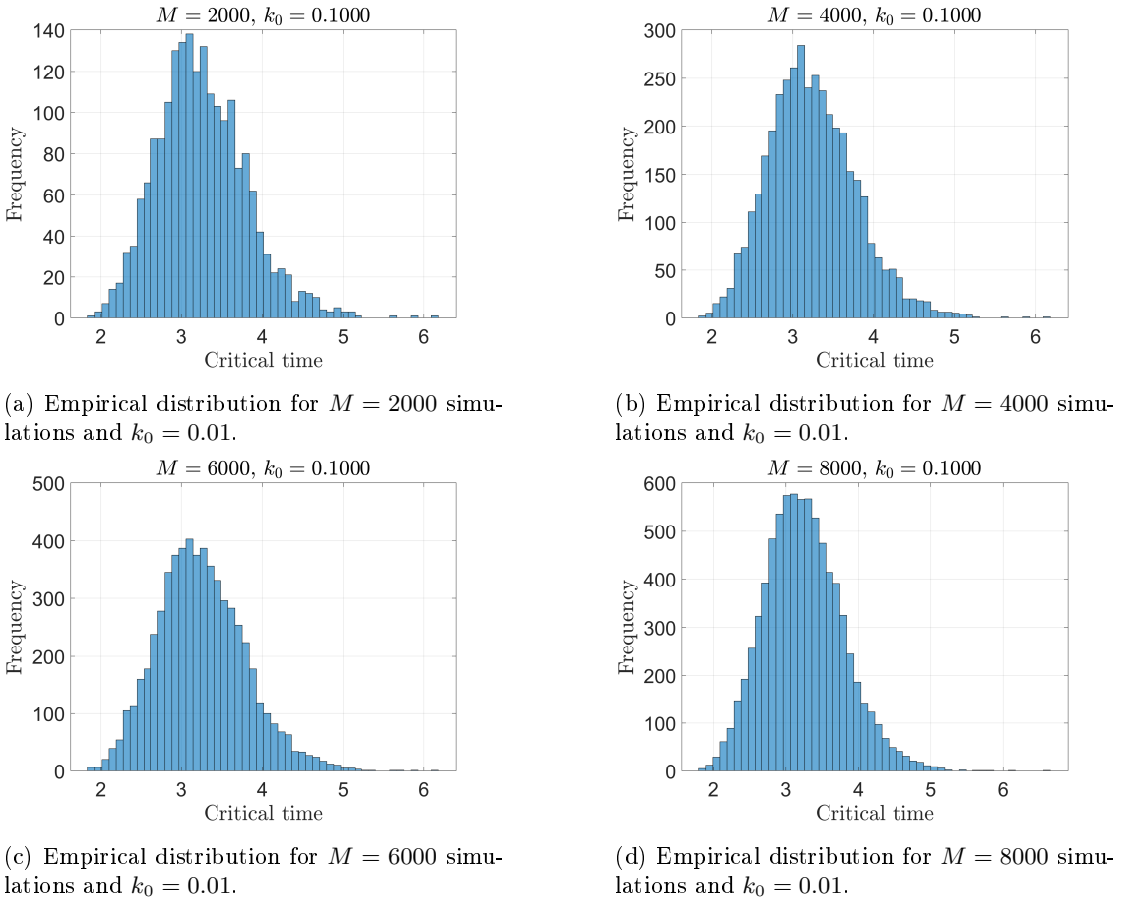


Figure 2: Empirical distributions of the critical time  $t_c$  for various numbers of simulations ( $M = 2000$ ,  $M = 4000$ ,  $M = 6000$ , and  $M = 8000$ ) with  $k_0 = 0.01$ .

$M$	$\mu$	$\sigma$	$\gamma_1$	$\gamma_2$	$JB$	$p$	Normality
2000	3.2524	0.55061	0.55696	3.7904	155.46	0	Not normal
4000	3.2478	0.53432	0.39982	3.2491	116.91	$4.44 \times 10^{-16}$	Not normal
6000	3.2534	0.53438	0.41406	3.5842	256.76	$3.33 \times 10^{-16}$	Not normal
8000	3.2468	0.53302	0.36071	3.2222	189.95	$1.11 \times 10^{-16}$	Not normal

Table 1: Results of normality tests for the critical time  $t_c$  across varying  $M$ .

Here  $M$  is the number of simulations,  $\mu$  is the mean of the critical time  $t_c$ ,  $\sigma$  is the standard deviation of  $t_c$ ,  $\gamma_1$  the skewness of the distribution,  $\gamma_2$  the Kurtosis of the distribution,  $JB$  the Jarque-Bera test statistic,  $p$ :  $p$ -value for the Jarque-Bera test and normality indicates whether the distribution is normal based on the test.

The normality tests for the critical time  $t_c$  is conducted across varying numbers of simulations

( $M = 2000, 4000, 6000$ , and  $8000$ ). The mean ( $\mu$ ), defined as

$$\mu = \frac{1}{M} \sum_{i=1}^M t_c^{(i)}, \quad (3.8)$$

represents the average critical time, and remained stable around  $\mu \approx 3.25$ . The standard deviation ( $\sigma$ ), given by

$$\sigma = \sqrt{\frac{1}{M} \sum_{i=1}^M (t_c^{(i)} - \mu)^2}, \quad (3.9)$$

measures the variability of  $t_c$ , which was approximately  $\sigma \approx 0.53$  across all  $M$ . The skewness

$$\gamma_1 = \frac{\frac{1}{M} \sum_{i=1}^M (t_c^{(i)} - \mu)^3}{\sigma^3} \quad (3.10)$$

quantifies the asymmetry of the distribution, with positive values indicating a right-skewed distribution. In all cases,  $\gamma_1$  is positive but globally decreases as  $M$  increases (for  $M = 6000$  the pattern changes). The kurtosis

$$\gamma_2 = \frac{\frac{1}{M} \sum_{i=1}^M (t_c^{(i)} - \mu)^4}{\sigma^4}, \quad (3.11)$$

measures the tailedness of the distribution, with values slightly exceeding 3, suggesting a leptokurtic behavior. Finally, the *Jarque-Bera test*, defined as

$$JB = \frac{M}{6} \left( \gamma_1^2 + \frac{(\gamma_2 - 3)^2}{4} \right), \quad (3.12)$$

combines skewness and kurtosis to test for normality. The  $p$ -value for the Jarque-Bera test is calculated using the chi-squared distribution with 2 degrees of freedom:  $p = 1 - F_{\chi^2}(JB; 2)$ . For all values of  $M$ , the  $p$ -value is nearly zero, leading to a rejection of the null hypothesis of normality. These results indicate that the distribution of  $t_c$  deviates significantly from normality, showing both skewness and heavier tails. The analysis leads to the conclusion of non statistical normality.

### 3.2. The viscous problem

In this section we analyze the case in which  $\nu > 0$ . For this purpose, we start analyzing the heat equation as a stepping stone to deriving the solution of Burgers equation via the Cole-Hopf transformation [3]. Consider the following heat equation with initial profile,

$$\begin{cases} w_t - \nu w_{xx} = 0, \\ w(x, 0) = 1 + \sum_{i=1}^N \sqrt{2S(k_i)\Delta k} \cos(k_i x + \varphi_i), \end{cases} \quad (3.13)$$

where

$$S(k) = Q e^{-\frac{(k-k_0)^2}{4K^2}}, \quad k_i = i\Delta k, \quad \varphi_i \sim \mathcal{U}[0, 2\pi]. \quad (3.14)$$

Using the Cole-Hopf transformation, the solution to Burger's equation,

$$u_t + uu_x - \nu u_{xx} = 0, \quad (3.15)$$

can be derived from the solution of the heat equation. The Cole-Hopf transformation relates the solutions of these two equations through the relationship

$$u(x, t) = -2\nu \frac{w_x(x, t)}{w(x, t)}. \quad (3.16)$$

Specifically, setting

$$w(x, t) = e^{\alpha\phi(x, t)}, \quad \alpha \neq 0, \quad (3.17)$$

we have that

$$\frac{\partial \phi}{\partial t} = \nu \frac{\partial^2 \phi}{\partial x^2} + \nu \alpha \left( \frac{\partial \phi}{\partial x} \right)^2. \quad (3.18)$$

Taking the derivative with respect to  $x$  and letting  $u = \phi_x$ , we obtain Burger's equation:

$$\frac{\partial u}{\partial t} + u \frac{\partial u}{\partial x} = \nu \frac{\partial^2 u}{\partial x^2}, \quad (3.19)$$

for  $\alpha = -(2\nu)^{-1}$ . For further details, refer to [14, 3]. The solution to the heat equation for the given initial condition is

$$w(x, t) = 1 + \sum_{i=1}^N \sqrt{2Qe^{-\frac{(k_i-k_0)^2}{4K^2}} \Delta k} \cos(k_i x + \varphi_i) e^{-\nu k_i^2 t}. \quad (3.20)$$

Using the Cole-Hopf transformation, the corresponding solution to Burger's equation is

$$u(x, t) = -2\nu \frac{w_x(x, t)}{w(x, t)} = 2\nu \left( \frac{\sum_{i=1}^N k_i \sqrt{2Qe^{-\frac{(k_i-k_0)^2}{4K^2}} \Delta k} \sin(k_i x + \varphi_i) e^{-\nu k_i^2 t}}{1 + \sum_{i=1}^N \sqrt{2Qe^{-\frac{(k_i-k_0)^2}{4K^2}} \Delta k} \cos(k_i x + \varphi_i) e^{-\nu k_i^2 t}} \right). \quad (3.21)$$

For the general case of Burger's equation with initial condition  $u(x, 0) = u_0(x)$ , the initial data can be expressed as

$$u_0(x) = -2\nu \frac{w_x(x, 0)}{w(x, 0)}. \quad (3.22)$$

By separating variables, the initial condition for the heat equation becomes

$$w(x, 0) = \exp \left( -\frac{1}{2\nu} \int_0^x u_0(s) ds \right). \quad (3.23)$$

The solution to the heat equation with this initial condition is

$$w(x, t) = \int_{-\infty}^{\infty} f(\eta) \frac{1}{\sqrt{4\pi\nu t}} e^{-\frac{(x-\eta)^2}{4\nu t}} d\eta, \quad (3.24)$$

where  $f(\eta) = w(\eta, 0)$ . Finally, the solution to Burger's equation is

$$u(x, t) = \frac{\int_{-\infty}^{\infty} f(\eta) \left( \frac{x-\eta}{t} \right) e^{-\frac{(x-\eta)^2}{4\nu t}} d\eta}{\int_{-\infty}^{\infty} f(\eta) e^{-\frac{(x-\eta)^2}{4\nu t}} d\eta}. \quad (3.25)$$

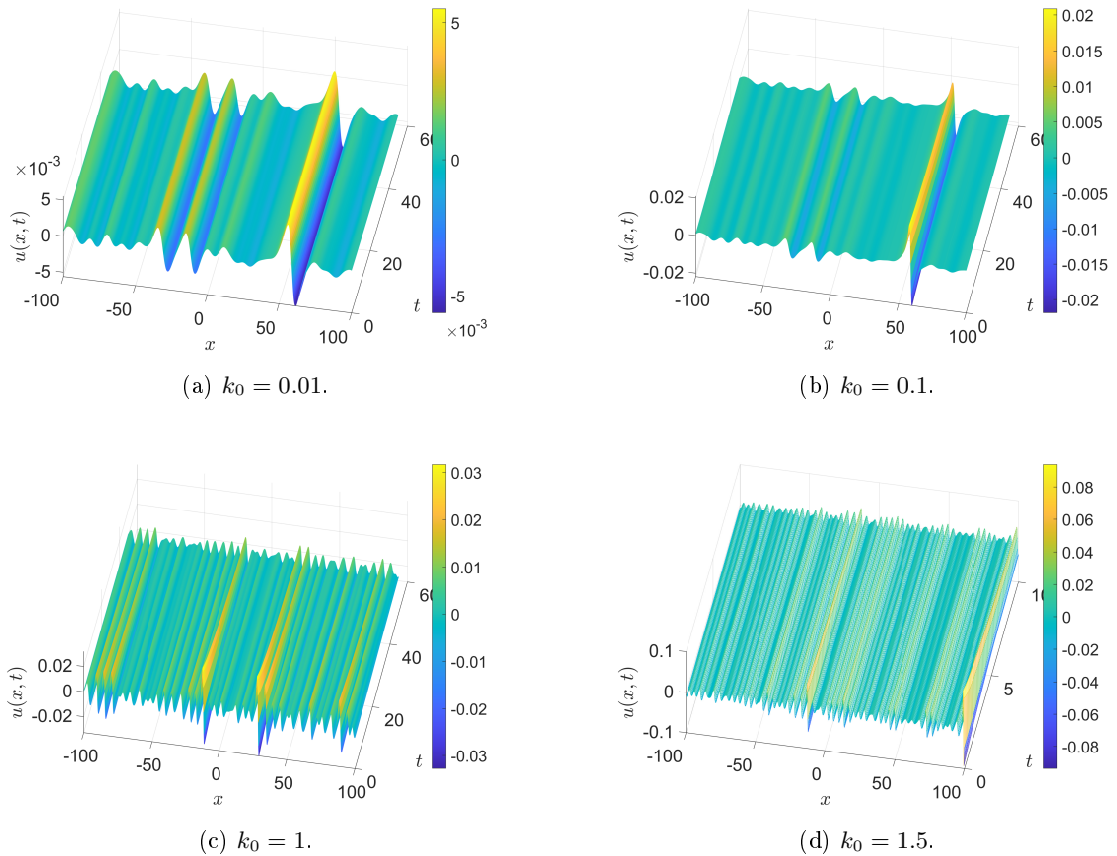


Figure 3: Plots of  $u(x, t)$  for different spatial domains and time horizons (adapted to see the asymptotic behavior) derived using the Cole-Hopf technique. The subfigures correspond to  $k_0 = 0.01$ ,  $k_0 = 0.1$ ,  $k_0 = 1$ , and  $k_0 = 1.5$ , respectively.

Figures 3a-3d show that over time, the wave amplitudes decrease to zero in all cases, a behavior attributed to exponential decay. Moreover, it is evident that the decay rate is faster for larger values of  $k_0$ . Simulations for  $k_0 > 2$  were performed, and we observed that, for instance, when  $k_0 = 10$ , the amplitude decreased to  $10^{-59}$  when  $t$  was close to 0.

### 3.3. The forced stochastic Burgers equation

Many authors have leveraged the fact that, with an appropriate change of variables, dispersive equations with quadratic nonlinearity of the form  $uu_x$  and a stochastic forcing term can be transformed into equations with constant coefficients [8, 11, 12, 24]. To illustrate this, consider a forced Burgers equation with a forcing term  $\psi(t)$ :

$$u_t + uu_x - \nu u_{xx} = \psi(t), \quad x \in \mathbb{R}, \quad t \in (0, \infty). \quad (3.26)$$

We first introduce a new variable  $\eta(x, t)$  defined as:

$$\eta(x, t) = u(x, t) + Z(t), \quad \text{where } Z'(t) = \psi(t). \quad (3.27)$$

Substituting (3.27) into the original equation yields:

$$\eta_t + Z(t)\eta_x + \eta\eta_x - \nu\eta_{xx} = 0, \quad x \in \mathbb{R}, \quad t \in (0, \infty). \quad (3.28)$$

Next, we define a shifted spatial coordinate:

$$\tilde{x} = x - V(t), \quad \text{where } V'(t) = Z(t). \quad (3.29)$$

Transforming the equation to the new coordinate system and simplifying leads to the viscous Burgers equation with constant coefficients:

$$\eta_t + \eta\eta_x - \nu\eta_{xx} = 0, \quad x \in \mathbb{R}, \quad t \in (0, \infty). \quad (3.30)$$

When a forcing term  $\psi(t)$  is introduced, the solution  $u(x, t)$  can be therefore expressed as:

$$u(x, t) = \int_{t_0}^t \psi(s) ds + 2\nu \left( \frac{\sum_{i=1}^N k_i \sqrt{2Qe^{-\frac{(k_i-k_0)^2}{4K^2}} \Delta k} \sin(k_i(x - V(t)) + \varphi_i) e^{-\nu k_i^2 t}}{1 + \sum_{i=1}^N \sqrt{2Qe^{-\frac{(k_i-k_0)^2}{4K^2}} \Delta k} \cos(k_i(x - V(t)) + \varphi_i) e^{-\nu k_i^2 t}} \right), \quad (3.31)$$

where  $V''(t) = \psi(t)$ .

Notice that the term  $\psi$  does not influence the characteristics of the wave field; it only affects the pedestal. Meanwhile, the primary contribution to the wave field, according to the expression (3.31), comes from the phase. Therefore, to compute the averaged wave field, we assume that  $V(t)$  follows a uniform distribution,  $V(t) \sim \mathcal{U}[-\sigma(t), \sigma(t)]$ , where  $\sigma(t)$  is the dispersion parameter, which is a function of time. Consequently, the averaged wave field is computed as

$$\begin{aligned} \langle u \rangle &= \frac{1}{2\sigma(t)} \int_{-\sigma(t)}^{\sigma(t)} \left\{ \int_{t_0}^t \psi(s) ds + 2\nu \left( \frac{\sum_{i=1}^N k_i \sqrt{2Qe^{-\frac{(k_i-k_0)^2}{4K^2}} \Delta k} \sin(k_i(x - V(t)) + \varphi_i) e^{-\nu k_i^2 t}}{1 + \sum_{i=1}^N \sqrt{2Qe^{-\frac{(k_i-k_0)^2}{4K^2}} \Delta k} \cos(k_i(x - V(t)) + \varphi_i) e^{-\nu k_i^2 t}} \right) \right\} dV \\ &= \int_{t_0}^t \psi(s) ds - \frac{\nu}{\sigma(t)} \ln \left( \left| 1 + \sum_{i=1}^N \sqrt{2Qe^{-\frac{(k_i-k_0)^2}{4K^2}} \Delta k} \cos(k_i(x - V(t)) + \varphi_i) e^{-\nu k_i^2 t} \right| \right|_{-\sigma(t)}^{\sigma(t)} \\ &= \int_{t_0}^t \psi(s) ds - \frac{\nu}{\sigma(t)} \ln \left( \left| \frac{1 + \sum_{i=1}^N \sqrt{2Qe^{-\frac{(k_i-k_0)^2}{4K^2}} \Delta k} \cos(k_i(x - \sigma(t)) + \varphi_i) e^{-\nu k_i^2 t}}{1 + \sum_{i=1}^N \sqrt{2Qe^{-\frac{(k_i-k_0)^2}{4K^2}} \Delta k} \cos(k_i(x + \sigma(t)) + \varphi_i) e^{-\nu k_i^2 t}} \right| \right). \end{aligned} \quad (3.32)$$

An important consideration at this point is ensuring that the denominator

$$1 + \sum_{i=1}^N \sqrt{2Qe^{-\frac{(k_i-k_0)^2}{4K^2}} \Delta k} \cos(k_i(x + \sigma(t)) + \varphi_i) e^{-\nu k_i^2 t} \quad (3.33)$$

is never equal to zero. To achieve this, we bound the summation term:

$$\left| \sum_{i=1}^N \sqrt{2Qe^{-\frac{(k_i-k_0)^2}{4K^2}} \Delta k} \cos(k_i(x + \sigma(t)) + \varphi_i) e^{-\nu k_i^2 t} \right| \leq \sum_{i=1}^N \sqrt{2Qe^{-\frac{(k_i-k_0)^2}{4K^2}} \Delta k}. \quad (3.34)$$

Thus, to ensure that

$$1 > \sum_{i=1}^N \sqrt{2Qe^{-\frac{(k_i-k_0)^2}{4K^2}} \Delta k}, \quad (3.35)$$

it is sufficient to require that  $N \cdot \sqrt{Q\Delta k} < 1$ . Note that this is not a necessary condition, as the cosine term oscillates. However, this condition provides a sufficient guarantee that the denominator never equals zero. Empirically, we observe that, even for  $N \cdot \sqrt{Q\Delta k} \geq 1$ , the denominator remains different from zero.

In order to interpret the solution we need to fix a set of parameters. To this end, we choose initially  $k_0 = 0.1$ , which represent long waves and  $\nu = 0.1$  for Reynolds viscosity. Figures 4a-4d displays the evolution of the averaged wave field for different values of the dispersion parameter. The effect of the random phase on the averaged solution is clear. The wave field tend to spread and damping over time. This behaviour is similar to the case of soliton solutions discussed in [12, 10]. The same can be observed for a time dependent dispersion, see Figures 5a-5d.

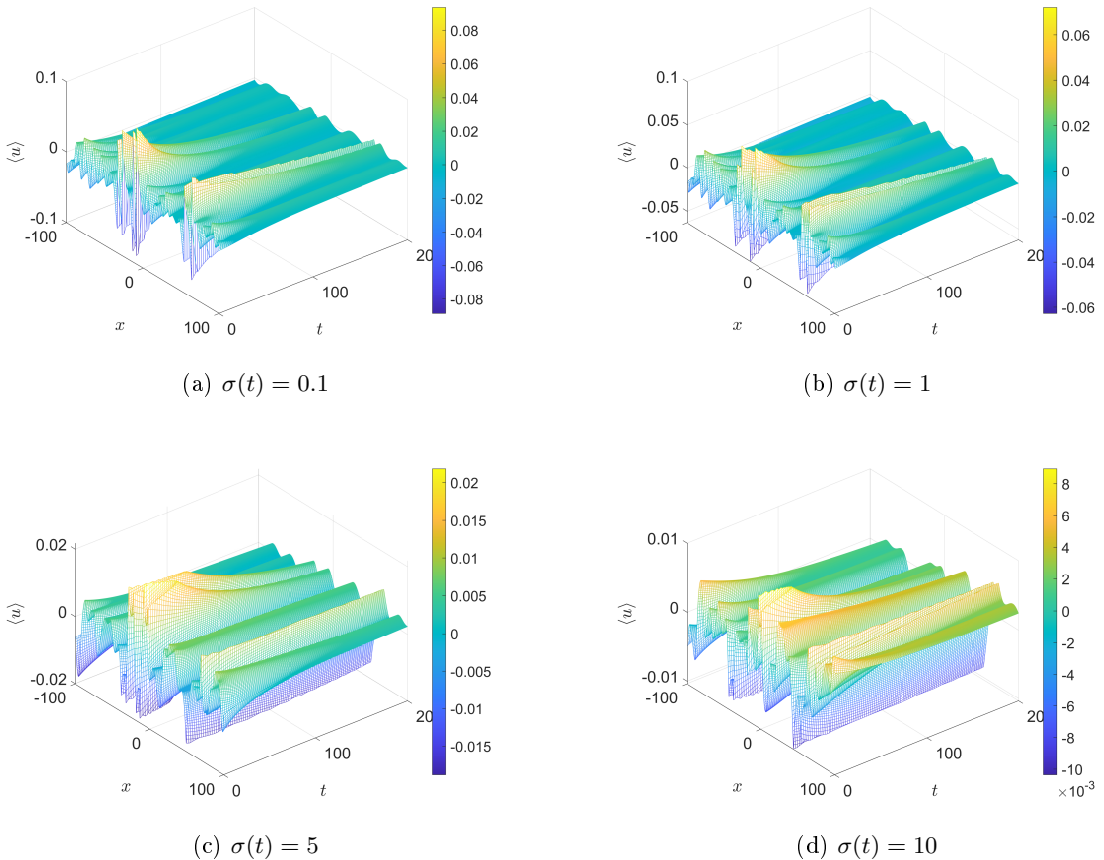


Figure 4: Plots of  $u(x, t)$  for different values of  $\sigma(t)$ :  $\sigma(t) = 1$ ,  $\sigma(t) = 5$ ,  $\sigma(t) = 10$ , and  $\sigma(t) = 20$ . Time scale adjusted to see convergence when  $t \rightarrow \infty$ .

For a non-time-homogeneous  $\sigma(t)$ , it is observed that the more convex  $\sigma(t)$  is, the faster the decay of the amplitude. Specifically, as shown in Figure 5b, the amplitude decreases more rapidly for  $\sigma(t) = t^2$ . Conversely, for  $\sigma(t) = \ln(t + 1)$  (Figure 5d), the decrease is slower and less pronounced.

The transformations introduced allow us to convert the forced Burgers equation into a form with constant coefficients, simplifying the analysis. The inclusion of a forcing term introduces a dependency on  $\psi(t)$  and  $V(t)$ , whose statistical properties significantly influence the behavior of

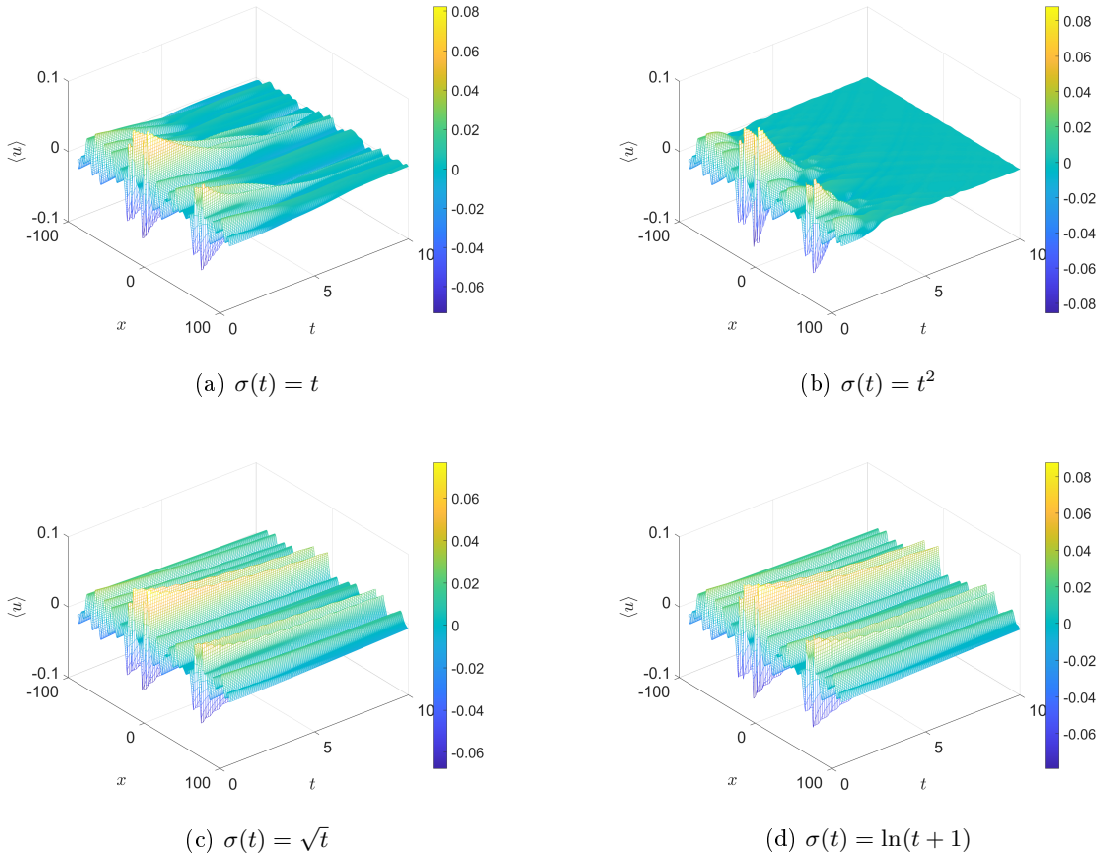


Figure 5: Plots of  $u(x, t)$  for different values of  $\sigma(t)$ :  $\sigma(t) = t$ ,  $\sigma(t) = t^2$ ,  $\sigma(t) = \sqrt{t}$ , and  $\sigma(t) = \ln(t + 1)$ .

the solution.

## 4. Conclusions

In this work, we investigated irregular wave fields described by the Burgers equation. For the inviscid case, we computed the averaged wave-breaking time and empirically demonstrated that it closely follows a normal distribution, yet the statistical tests reject normality. For the viscous case, exact solutions were obtained using the Cole-Hopf transformation, which were then utilized to study the problem under a random external force. The forced problem was addressed by introducing a change of variables that transformed the stochastic Burgers equation into a deterministic one. We demonstrated that randomness primarily affects the phase of the solution. By assuming it follows a uniform distribution, we showed that the averaged wave field tends to spread and dampen over time.

## Declarations

### Conflict of interest

The authors state that there is no conflict of interest.

### Data availability

Data sharing is not applicable to this article as all parameters used in the numerical experiments are informed in this paper.

## References

- [1] Alhejaili, W.; Roy, S.; Raut, S.; Roy, A.; Salas, AH.; Aboelenen, T.; El-Tantawy, SA. Analytical solutions to (modified) Korteweg–de Vries–Zakharov–Kuznetsov equation and modeling ion-acoustic solitary, periodic, and breather waves in auroral magnetoplasmas. *Phys. Plasmas.* **2024**, *31*, 082107.
- [2] Benjamin, T.B. Internal waves of permanent form of great depth. *J Fluid. Mech.* **1967**, *295*, 381-394.
- [3] Burgers, J.M. The nonlinear diffusion equation—Asymptotic solutions and statistical problems. *Springer.* **1974**.
- [4] Cao, N.; Yin X.J.; Bai, S.; Xu, LY. Lump-soliton, rogue-soliton interaction solutions of an evolution model for magnetized Rossby waves. *Nonlinear Dyn.* **2024**, *112*, 9367-9389.
- [5] Chadha NM.; Tomar, S.; Raut, S.; Parametric analysis of dust ion acoustic waves in superthermal plasmas through non-autonomous KdV framework. *Communications in Non-linear Science and Numerical Simulation.* **2023**, *123*, 107269.
- [6] Flamarion, M.V.; Pelinovsky E. Soliton interactions with an external forcing: the modified Korteweg-de Vries framework. *Chaos, Solitons & Fractals.* **2022**, *165*, 112889.
- [7] Flamarion, M.V. Trapped waves generated by an accelerated moving disturbance for the Whitham equation. *Partial Differential Equations in Applied Mathematics.* **2022**, *5*, 100356.
- [8] Flamarion, M.V.; Pelinovsky E. Makarov, D.V. Solitons in dissipative systems subjected to random force within the Benjamin-Ono type equation. *Chaos, Solitons & Fractals.* **2024**, *187*, 115373.
- [9] Flamarion, M.V.; Pelinovsky E. Wave fields under the influence of a random-driven force: The Burgers equation. *Phys Lett A.* **2024**, *527*, 130000.
- [10] Flamarion, M.V.; Pelinovsky E. Solitons in dissipative systems subjected to random force within the Benjamin-Ono type equation *Chaos, Soliton & Fractals* **2024**, *187*, 115373.
- [11] Gurbatov, S.N.; Pelinovskii, E.N.; Saichev, A.I. Problem of closure of the equations for the averaged fields in nonlinear media containing chaotic inhomogeneities. *Radiophys Quantum Electron.* **1978**, *21*, 1032-1037.

- [12] Pelinovsky, E.; Sergeeva, A. KdV-Soliton dynamics in a random field *Radiophys. Quantum Electron.* **2006**, 49(7): 540-546.
- [13] Pelinovsky, E.; Talipova, T.; Didenkulova, E. The Hopf equation with certain modular nonlinearities *Physics Letters A.* **2024**, 507, 129489.
- [14] Salih, A. Burgers' Equation. *Lecture notes, Department of Aerospace Engineering, Indian Institute of Space Science and Technology, Thiruvananthapuram.* 18 February 2016.
- [15] Raut, S.; Roy, S.; Kairi, R.R.; Chatterjee, P. Approximate Analytical Solutions of Generalized Zakharov–Kuznetsov and Generalized Modified Zakharov–Kuznetsov Equations. *Int. J. Appl. Comput. Math.* **2021**, 7, 157.
- [16] Raut, S.; Roy, S.; Saha, S.; Das, A.N. Studies on the Dust–Ion–Acoustic Solitary Wave in Planar and Non-Planar Super-Thermal Plasmas with Trapped Electrons. *Plasma Phys. Rep.* **2022**, 48, 627-637.
- [17] Raut, S.; Mondal, K.K.; Chatterjee, P.; Roy, S. Dust ion acoustic bi-soliton, soliton, and shock waves in unmagnetized plasma with Kaniadakis-distributed electrons in planar and nonplanar geometry. *Eur. Phys. J. D* **2023**, 77, 100.
- [18] Roy, A.; Mondal, K.K.; Chatterjee, P.; Raut, S. Influence of External Periodic Force On Ion Acoustic Waves in a Magnetized Dusty Plasma Through Forced KP Equation and Modified Forced KP Equation. *Braz J Phys.* **2022**, 52, 65.
- [19] Porter, A.; Smyth, N. Modelling the morning glory of the Gulf of Carpentaria. *J Fluid Mech.* **2002**, 454, 1-20.
- [20] Smyth, NF.; Holloway, PE. Hydraulic jump and undular bore formation on a shelf break. *J. Phys. Oceanogr.* **1988**, 18, 947-962.
- [21] Vargas-Magaña RM.; Marchant, TR.; Smyth, N. Numerical and analytical study of undular bores governed by the full water wave equations and bidirectional Whitham-Boussinesq equations. *Phys Fluids.* **2021**, 33, 067105.
- [22] Whitham, G.B. Linear and Nonlinear Waves John Wiley & Sons, Inc, New York. **1974**.
- [23] Zabusky, M.; Kruskal, N. Interaction of solitons in a collisionless plasma and the recurrence of initial states. *Phys Rev Lett.* **1965**, 15, 240-243.
- [24] Zahibo, N.; Pelinovsky, E.; Sergeeva, A. Weakly damped KdV soliton dynamics with the random force *Chaos Solitons & Fractals.* **2009**, 39, 1645-1650.